

Stable Autoencoding: A Flexible Framework for Regularized Low-Rank Matrix Estimation

Julie Josse
Department of Applied Mathematics
Agrocampus Ouest
Rennes, France
josse@agrocampus-ouest.fr

Stefan Wager
Department of Statistics
Stanford University
Stanford, U.S.A.
swager@stanford.edu

December 7, 2024

Abstract

We develop a framework for low-rank matrix estimation that allows us to transform noise models into regularization schemes via a simple parametric bootstrap. Effectively, our procedure seeks an autoencoding basis for the observed matrix that is robust with respect to the specified noise model. In the simplest case, with an isotropic noise model, our procedure is equivalent to a classical singular value shrinkage estimator. For non-isotropic noise models, however, our method does not reduce to singular value shrinkage, and instead yields new estimators that perform well in experiments. Moreover, by iterating our stable autoencoding scheme, we can automatically generate low-rank estimates without specifying the target rank as a tuning parameter.

KEYWORDS: Artificial data corruption, correspondence analysis, parametric bootstrap.

1 Introduction

Low-rank matrix estimation plays a key role in many scientific and engineering tasks, including collaborative filtering [Koren et al., 2009], genome-wide studies [Leek and Storey, 2007, Price et al., 2006], and magnetic resonance imaging [Candès et al., 2013, Lustig et al., 2008]. Low-rank procedures are often motivated by the following statistical model. Suppose that we observe a noisy matrix $X \in \mathbb{R}^{n \times p}$ drawn from some distribution $\mathcal{L}(\mu)$ with $\mathbb{E}_\mu[X] = \mu$, and that we have scientific reason to believe that μ admits a parsimonious,

low-rank representation. Then, we can frame our statistical goal as trying to recover the underlying μ from the observed X . Candès and Tao [2010], Chatterjee [2014], Shabalin and Nobel [2013], Gavish and Donoho [2014b], and others have studied regimes where it is possible to accurately do so.

Classical approaches to estimating μ from X are centered around singular-value decomposition (SVD) algorithms. Let

$$X = \sum_{l=1}^{\min\{n,p\}} u_l d_l v_l^\top \quad (1)$$

denote the SVD of X .¹ Then, if we believe that μ should have rank k , the standard SVD estimator $\hat{\mu}_k$ for μ is

$$\hat{\mu}_k = \sum_{l=1}^k u_l d_l v_l^\top. \quad (2)$$

In other words, we estimate μ using the closest rank- k approximation to X . Often, however, the plain rank- k estimator (2) is found to be noisy, and its performance can be improved by regularization. Existing approaches to regularizing $\hat{\mu}_k$ focus on singular value shrinkage, and use

$$\hat{\mu}^{\text{shrink}} = \sum_{l=1}^{\min\{n,p\}} u_l \psi(d_l) v_l^\top, \quad (3)$$

where ψ is a shrinkage function that is usually chosen in a way that makes $\hat{\mu}^{\text{shrink}}$ the closest to μ according to a loss function. Several authors have proposed various choices for ψ [e.g., Candès et al., 2013, Chatterjee, 2014, Josse and Sardy, 2014, Verbanck et al., 2013, Shabalin and Nobel, 2013, Gavish and Donoho, 2014a].

Methods based on singular-value shrinkage have achieved considerable empirical success. They also have provable optimality properties in the Gaussian noise model where $X = \mu + \varepsilon$ and the ε_{ij} are independent and identically distributed Gaussian noise terms [Shabalin and

¹Recall that, in the SVD, the $\{u_l\}$ and $\{v_l\}$ form orthogonal sets, and the d_l form a decreasing non-negative sequence.

Nobel, 2013]. However, in the non-Gaussian case, mere singular-value shrinkage can prove to be limiting, and we may also need to rotate the singular vectors u_l and v_l in order to achieve good performance.

In this paper, we propose a new framework for regularized low-rank estimation that does not start from the singular-value shrinkage point of view. Our approach is motivated by a simple parametric bootstrap idea [Efron and Tibshirani, 1993]. It is well known that the classical SVD estimator $\hat{\mu}_k$ can be written as [Boulevard and Kamp, 1988, Baldi and Hornik, 1989]

$$\hat{\mu}_k = XB_k, \text{ where } B_k = \operatorname{argmin}_B \left\{ \|X - XB\|_2^2 : \operatorname{rank}(B) \leq k \right\}. \quad (4)$$

The matrix B , called a linear *autoencoder* of X , allows us to encode the features of X using a low-rank representation.

Now, in the context of our noise model $X \sim \mathcal{L}(\mu)$, we do not just want to compress X and instead want to recover μ from X . From this perspective, we would much prefer to estimate μ using an oracle encoder matrix that formally provides the best linear approximation of μ given our noise model

$$\hat{\mu}_k^* = XB_k^*, \text{ where } B_k^* = \operatorname{argmin}_B \left\{ \mathbb{E}_{X \sim \mathcal{L}(\mu)} \left[\|\mu - XB\|_2^2 \right] : \operatorname{rank}(B) \leq k \right\}. \quad (5)$$

We of course cannot solve for B_k^* because we do not know μ . But we can estimate B_k^* using a parametric bootstrap where we replace μ in (5) by any guess $\hat{\mu}^0(X)$ for μ .

A first possibility is to use X as our initial estimate for μ , i.e., set $\hat{\mu}^0(X) = X$, resulting in an estimator

$$\hat{\mu}_k^{\text{stable}} = X\hat{B}_k, \text{ where } \hat{B}_k = \operatorname{argmin}_B \left\{ \mathbb{E}_{\tilde{X} \sim \mathcal{L}(X)} \left[\|X - \tilde{X}B\|_2^2 \right] : \operatorname{rank}(B) \leq k \right\}. \quad (6)$$

We call this choice of \hat{B}_k a *stable autoencoder* of X , as it provides a parsimonious encoding of the features of X that is stable when perturbed with noise of the form $\mathcal{L}(\cdot)$. In the classical

isotropic Gaussian case $X = \mu + \varepsilon$, the estimator $\hat{\mu}_k^{\text{stable}}$ reduces to a classical singular-value shrinkage estimator, as shown in Section (2). However, Gaussian noise models are not always appropriate. For example, if X contains many zeros, we can use a random blackout model $X_{ij} = Z_{ij}(\mu_{ij} + \varepsilon_{ij})$, where ε_{ij} is Gaussian noise and $Z_{ij} \sim \pi^{-1}\text{Bernoulli}(\pi)$ sets some coordinates to zero. Or, if X contains count data, it may be appropriate to use a Poisson noise model $X_{ij} = \text{Poisson}(\mu_{ij})$. With these alternative noise models, the framework (6) yields new estimators for μ that can perform better than methods based on singular value shrinkage.

One difficulty with the estimator $\hat{\mu}_k^{\text{stable}}$ is that we need to select the rank k of the estimator beforehand. Surprisingly, we can get around this issue by iterating the optimization problem (6) until we converge to a fixed point

$$\hat{\mu}^{\text{iter}} = X\hat{B}, \text{ where } \hat{B} = \underset{B}{\operatorname{argmin}} \left\{ \mathbb{E}_{\tilde{X} \sim \mathcal{L}(\hat{\mu}^{\text{iter}})} \left[\left\| \hat{\mu}^{\text{iter}} - \tilde{X}B \right\|_2^2 \right] \right\}. \quad (7)$$

As we show in Section 3, the iterative algorithm implied by this estimator converges to a low-rank fixed point. In our experiments, this *iterated stable autoencoder* does a good job at estimating k of the underlying signal; thus, all the statistician needs to do is to specify a noise model $\mathcal{L}(\cdot)$.

Our method appears to be particularly useful for working with count data, as then we have a natural non-Gaussian model for $\mathcal{L}(\cdot)$, namely a Poisson or binomial model. In Section 4, we show how to use our method to regularize correspondence analysis [Greenacre, 1984, 2007], which is one of the most popular ways to analyze multivariate count data.

To summarize, our parametric bootstrap framework as instantiated in (6) and (7) provides us with a flexible framework for transforming noise models $\mathcal{L}(\cdot)$ into regularized matrix estimators. In the Gaussian case, our framework yields estimators that resemble best-practice singular-value shrinkage methods. Meanwhile, in the non-Gaussian case, stable

autoencoding allows us to learn new singular vectors for $\hat{\mu}$. In our experiments, this allowed us to substantially improve over existing techniques.

1.1 Related Work

There is a well-known duality between regularization and feature noising schemes. As shown by Bishop [1995], linear regression with features perturbed with Gaussian noise, i.e.,

$$\hat{\beta} = \operatorname{argmin}_{\beta} \left\{ \mathbb{E}_{\varepsilon_{ij} \stackrel{\text{iid}}{\sim} \mathcal{N}(0, \sigma^2)} \left[\|Y - (X + \varepsilon) \beta\|_2^2 \right] \right\},$$

is equivalent to ridge regularization with Lagrange parameter $\lambda = n\sigma^2$:

$$\hat{\beta}_{\lambda}^{(R)} = \operatorname{argmin}_{\beta} \left\{ \|Y - X\beta\| + \lambda \|\beta\|_2^2 \right\}.$$

Because ridge regression is equivalent to adding homoscedastic noise to X , we can think of ridge regression as making the estimator robust against round perturbations to the data.

However, if we perturb the features X using non-Gaussian noise or are working with a non-quadratic loss function, artificial feature noising can yield new regularizing schemes with desirable properties [Globerson and Roweis, 2006, Simard et al., 2000, van der Maaten et al., 2013, Wager et al., 2013, Wang et al., 2013]. Our proposed estimator $\hat{\mu}_k^{\text{stable}}$ can be seen as an addition to this literature, as we seek to regularize $\hat{\mu}_k$ by perturbing the autoencoder optimization problem.

The idea of regularizing via feature noising is also closely connected to the dropout learning algorithm for training neural networks [Srivastava et al., 2014], which aims to regularize a neural network by randomly omitting hidden nodes during training time. Dropout and its generalizations have been found to work extremely well in many large-scale prediction tasks [e.g., Baldi and Sadowski, 2014, Goodfellow et al., 2013, Krizhevsky et al., 2012].

2 Fitting Stable Autoencoders

In this section, we show how to solve (6) under various noise models $\mathcal{L}(\cdot)$. This provides us with estimators $\hat{\mu}^{\text{stable}}$ that are interesting in their own right, and also serves as a stepping stone to the iterative solutions from Section 3 that do not require specifying the rank k of the underlying signal.

2.1 Isotropic Stable Autoencoders and Singular-Value Shrinkage

At first glance, the estimator $\hat{\mu}_k^{\text{stable}}$ defined in (6) may seem like a surprising idea. It turns out, however, that under the isotropic Gaussian² noise model

$$X = \mu + \varepsilon, \text{ with } \varepsilon_{ij} \stackrel{\text{iid}}{\sim} \mathcal{N}(0, \sigma^2) \text{ for all } i = 1, \dots, n \text{ and } j = 1, \dots, p, \quad (8)$$

$\hat{\mu}_k^{\text{stable}}$ is equivalent to a classical singular-value shrinkage estimator (3) with $\psi(d) = d/(1 + \lambda/d^2)$.

Theorem 1. *Let $\hat{\mu}_k^{\text{stable}}$ be the rank- k estimator for μ induced by the stable autoencoder (6) with noise model $\mathcal{L}(\cdot)$ as defined in (8) with some $\sigma \geq 0$. This estimator can also be written as the solution to a ridge-regularized autoencoder:*

$$\hat{\mu}_k^{\text{stable}} = X \hat{B}_k, \text{ where } \hat{B}_k = \operatorname{argmin}_B \left\{ \|X - XB\|_2^2 + \lambda \|B\|_2^2 : \operatorname{rank}(B) \leq k \right\} \quad (9)$$

with $\lambda = n\sigma^2$. Moreover, using notation from (1), we can write $\hat{\mu}_k^{\text{stable}}$ as

$$\hat{\mu}_k^{\text{stable}} = \sum_{l=1}^k u_l \frac{d_l}{1 + \lambda/d_l^2} v_l^\top. \quad (10)$$

In the isotropic Gaussian noise case, singular-value shrinkage methods were shown by Shabalin and Nobel [2013] to have strong optimality properties for estimating μ . Thus, it

²Theorem 1 holds for all isotropic noise models with $\operatorname{Var}[\varepsilon_{ij}] = \sigma^2$ for all i and j , and not just the Gaussian one. However, in practice, isotropic noise is almost always modeled as Gaussian.

is reassuring that our framework recovers an estimator of this class in the Gaussian case. In fact, the induced shrinkage function resembles a first-order approximation to the one proposed by Verbanck et al. [2013].

We note that, when $\sigma \neq 0$, our estimator is not invariant to transposition $X \rightarrow X^\top$ because λ depends on n but not on p . The reason for this discrepancy is that, if $n > p$, the rows of X are more perturbed by the extra noise than the columns of X . For example, we can check that

$$\sum_{j=1}^p \mathbb{E}_{\tilde{X} \sim \mathcal{L}(X)} \left[u_1 \cdot \tilde{X}_{.j} \right]^2 = d_1^2 \quad \text{and} \quad \sum_{j=1}^p \text{Var}_{\tilde{X} \sim \mathcal{L}(X)} \left[u_1 \cdot \tilde{X}_{.j} \right] = p\sigma^2,$$

and so the signal-to-noise ratio from our artificial noising along the first singular column u_1 is $d_1^2/p\sigma^2$; conversely, the signal-to-noise ratio along the first singular row v_1 is $d_1^2/n\sigma^2$. Thus, when $n > p$, noising X will induce us to regularize more if we want to find a stable encoding of the rows of X instead of the columns of X (and vice-versa when $n < p$). In our experiments, we usually obtained better results for estimating μ by transposing X such as to have $n \geq p$.

2.2 Non-Isotropic Stable Autoencoders

Stable autoencoders with isotropic noise are attractive in the sense that we can carefully analyze their behavior in closed form. However, from a practical point of view, our procedure is most useful outside of the isotropic regime, as it induces new estimators $\hat{\mu}$ that do not reduce to singular-value shrinkage. Even in the non-isotropic noise model, low-rank stable autoencoders can still be efficiently solved, as shown below.

Theorem 2. *For a generic noise model $\mathcal{L}(\cdot)$, the matrix \hat{B}_k from (6) can be obtained as*

follows:

$$\hat{B}_k = \operatorname{argmin}_B \left\{ \|X - XB\|_2^2 + \left\| S^{\frac{1}{2}} B \right\|_2^2 : \operatorname{rank}(B) \leq k \right\}, \quad (11)$$

where S is a $p \times p$ diagonal matrix with

$$S_{jj} = \sum_{i=1}^n \operatorname{Var}_{\tilde{X} \sim \mathcal{L}(X)} [\tilde{X}_{ij}]. \quad (12)$$

From a computational point of view, we can write the solution \hat{B}_k of (11) as

$$\hat{B}_k = \operatorname{argmin}_B \left\{ \operatorname{tr} \left((B - \hat{B})^\top (X^\top X + S) (B - \hat{B}) \right) : \operatorname{rank}(B) \leq k \right\}, \text{ where} \quad (13)$$

$$\hat{B} = (X^\top X + S)^{-1} X^\top X \quad (14)$$

is the solution of (11) without the rank constraint.

The optimization problem in (13) can be easily solved by taking the top k terms from the eigenvalue decomposition of $\hat{B}^\top (X^\top X + S) \hat{B}$; the matrix \hat{B}_k can then be recovered by solving a linear system [e.g., Takane, 2013]. Thus, despite what we might have expected, solving the low-rank constrained stable autoencoder problem (6) with a generic noise model is not substantially more computationally demanding than singular-value shrinkage. Note that in (14), the matrix S is not equal to a constant times the identity matrix due to the non-isotropic noise; that's why the resulting singular vectors of $\hat{\mu}_k^{\text{stable}} = X \hat{B}_k$ are not the ones of X .

3 Automatic Low-Rank Estimation with Iterated Stable Autoencoders

One shortcoming of the stable autoencoders discussed in the previous section is that we need to specify the rank k as a tuning parameter. Selecting the rank for multivariate methods is

Algorithm 1 Low-rank matrix estimation via iterated stable autoencoding.

```

 $\hat{\mu} \leftarrow X$ 
 $S_{jj} \leftarrow \sum_{i=1}^n \text{Var}_{\tilde{X} \sim \mathcal{L}(X)} [\tilde{X}_{ij}]$  for all  $j = 1, \dots, p$ 
while algorithm has not converged do
   $\hat{B} \leftarrow (\hat{\mu}^\top \hat{\mu} + S)^{-1} \hat{\mu}^\top \hat{\mu}$ 
   $\hat{\mu} \leftarrow X \hat{B}$ 
end while

```

often a difficult problem, and many heuristics are available in the literature [Jolliffe, 2002, Josse and Husson, 2011]. The stable autoencoding framework, however, induces a simple solution to the rank-selection problem. As we show in this section, iterating our estimation scheme from the previous automatically yields low-rank solutions.

At a high level, our goal is to find a solution to

$$\hat{\mu}^{\text{iter}} = X \hat{B}, \text{ where } \hat{B} = \underset{B}{\text{argmin}} \left\{ \mathbb{E}_{\tilde{X} \sim \mathcal{L}(\hat{\mu}^{\text{iter}})} \left[\left\| \hat{\mu}^{\text{iter}} - \tilde{X} B \right\|_2^2 \right] \right\}$$

by iteratively updating \hat{B} and $\hat{\mu}$. Using the unconstrained solution (14) from Theorem 2, we get the formal procedure described in Algorithm 1. Note that we do not update the matrix S , which encodes the variance of the noise distribution, and only update $\hat{\mu}$. As shown below, our algorithm converges to a well-defined solution; moreover, the solution is regularized in that $\hat{\mu}^\top \hat{\mu}$ is smaller than $X^\top X$ with respect to the positive semi-definite cone ordering.

Theorem 3. *Algorithm 1 converges to a fixed point $\hat{\mu} = X \hat{B}$. Moreover,*

$$\hat{\mu}^\top \hat{\mu} \preceq X^\top X.$$

The reason our algorithm converges to low-rank solutions is that our iterative scheme does not have any fixed points “near” low-dimensional subspaces. Specifically, as shown in Theorem 4, for any eigenvector of $\hat{\mu}^\top \hat{\mu}$, either $\|\hat{\mu} u\|_2$ must be larger than some cutoff, or it must be exactly zero. Thus, $\hat{\mu}$ cannot have any small but non-zero singular values. In our experiments, we have found that our algorithm in fact conservatively estimates the true

rank of the underlying signal.

Theorem 4. *Let $\hat{\mu}$ be the limit of our iterative algorithm, and let $u \in \mathbb{R}^p$ be any (normalized) eigenvector of $\mu^\top \mu$. Then, either*

$$\|\hat{\mu} u\|_2 = 0, \text{ or } \|\hat{\mu} u\|_2^2 \geq \frac{1}{\|XS^{-1}u\|_2^2}.$$

Finally we note that, in the isotropic case, our iterative algorithm again admits a closed-form solution. Looking at this solution can give us more intuition about what our algorithm does in the general case. In particular, we note that the algorithm never shrinks a singular value by more than a factor $1/2$ without pushing it all the way to 0.

Proposition 5. *In the isotropic case with $S = n\sigma^2 I$, our iterative algorithms converges to*

$$\hat{\mu}^{\text{iter}} = \sum_{l=1}^{\min\{n, p\}} u_l \psi(d_l) v_l^\top, \text{ where } \psi(d) = \begin{cases} \frac{1}{2} (d + \sqrt{d^2 - 4n\sigma^2}) & \text{for } d^2 \geq 4n\sigma^2, \\ 0 & \text{else.} \end{cases} \quad (15)$$

Since the isotropic Gaussian matrix estimation problem has been thoroughly studied, we can compare the shrinkage rule $\psi(\cdot)$ with known asymptotically optimal ones. Gavish and Donoho [2014b] provide a comprehensive treatment of optimal singular-value shrinkage under Marchenko-Pastur asymptotics, where n and p both diverge to infinity such that $n/p \rightarrow \beta$ for some $0 < \beta \leq 1$ while the rank and the scale of the signal remains fixed. The Marchenko-Pastur matrix asymptotic regime has been studied by, among others, Baik and Silverstein [2006], Johnstone [2001], and Paul [2007]

In what appears to be a remarkable coincidence, for the square case $\beta = 1$, our shrinkage rule (15) corresponds exactly to the Marchenko-Pastur optimal shrinkage rule under operator-norm loss; i.e., that it minimizes the limit of the operator norm of the matrix $(\hat{\mu} - \mu)$. At the very least, this connection is reassuring as it suggests that our iterative

scheme may yield statistically reasonable estimates $\hat{\mu}^{\text{iter}}$ for other noise models too. It remains to be seen whether this connection reflects a deeper theoretical phenomenon.

4 Regularizing Correspondence Analysis

When X contains count data, we have a natural noise model $X_{ij} \sim \text{Poisson}(\mu_{ij})$ for our data matrix X , and so our stable autoencoding framework is easy to apply. In this situation, however, X is often analyzed by correspondence analysis [Greenacre, 1984, 2007] rather than using a direct singular-value decomposition. Here, we show how to regularize correspondence analysis by stable autoencoding. This discussion also serves as a blueprint for extending our method to other low-rank multivariate techniques such as principal component analysis or canonical correlation analysis.

Correspondence analysis involves taking the singular-value decomposition of a transformed matrix M :

$$M = R^{-\frac{1}{2}} \left(X - \frac{1}{N} r c^\top \right) C^{-\frac{1}{2}}, \quad \text{where } R = \text{diag}(r), C = \text{diag}(c), \quad (16)$$

N is the the total number of counts and r and c are vectors containing the row and column sums of X . Once we have a rank- k estimate of \widehat{M}_k obtained as in (2), we get

$$\hat{\mu}_k^{CA} = R^{\frac{1}{2}} \widehat{M}_k C^{\frac{1}{2}} + \frac{1}{N} r c^\top. \quad (17)$$

Our goal is to get a better estimator \widehat{M} for the matrix M of the population; we then transform \widehat{M} into an estimate of μ using the same formula (17). Our framework requires first specifying a noise model. Since we are working with count data, we may want our estimator to be robust with respect to subsampling the observations used to construct the original matrix X . If we randomly delete each observation with probability $\delta \in (0, 1)$, we

get a noise model

$$\tilde{X}_{ij} \sim \frac{1}{1-\delta} \text{Binomial}(X_{ij}, 1-\delta) \quad (18)$$

A similar sampling scheme is known to work well for regularizing logistic regression with count features, and has desirable theoretical properties [Wager et al., 2014]. If we set $\delta = 0.5$, then this noising scheme yields the same regularized estimator as a parametric Poisson bootstrap.

Following (6), we propose estimating M as follows

$$\begin{aligned} \widehat{M}_k^{\text{stable}} &= M\widehat{B}_k, \text{ where} \\ \widehat{B}_k &= \operatorname{argmin}_B \left\{ \mathbb{E}_{\tilde{X} \sim \mathcal{L}(X)} \left[\left\| M - R^{-\frac{1}{2}} \left(\tilde{X} - \frac{1}{N} r c^\top \right) C^{-\frac{1}{2}} B \right\|_2^2 \right] : \operatorname{rank}(B) \leq k \right\}. \end{aligned} \quad (19)$$

Just as in Theorem 2, we can show that \widehat{B}_k solves

$$\widehat{B}_k = \operatorname{argmin}_B \left\{ \|M - MB\|_2^2 + \frac{\delta}{1-\delta} \|S_M^{\frac{1}{2}} B\| : \operatorname{rank}(B) \leq k \right\}, \quad (20)$$

where S_M is a diagonal matrix with $(S_M)_{jj} = c_j^{-1} \sum_{i=1}^n \operatorname{Var}[\tilde{X}_{ij}] / r_i$. We can efficiently solve for (20) using the same idea as in (13) and (14). Finally, if we do not want to fix the rank k , we can use an iterative scheme as in Section 3.

Interestingly, if we had chosen to sample \tilde{X} from an independent contingency table with

$$\mathbb{E}[\tilde{X}] = \frac{1}{N} r c^\top, \operatorname{Var}[\tilde{X}_{ij}] = \frac{\delta}{1-\delta} \frac{r_i c_j}{N}, \quad (21)$$

we would have obtained a regularization matrix $S_M = n\delta/(N(1-\delta))I_{p \times p}$. Because S_M is diagonal, the resulting estimator \widehat{M}_λ could then be obtained from M by singular value shrinkage. Thus, if we want to regularize correspondence analysis applied to a nearly independent table, singular value shrinkage based methods can achieve good performance; however, if the table has strong dependence, our framework provides a more principled way of being robust to sampling noise.

5 Simulation Experiments

To assess our proposed methods, we first ran comparative simulation studies for different noise models. We begin with a sanity check: in Section 5.1, we reproduce the isotropic Gaussian-noise experiments of Candès et al. [2013], and find that our method is competitive with existing approaches on this standard benchmark.

We then move to the non-isotropic case, where we can take advantage of our method’s ability to adapt to different noise structures. In Section 5.2 we show results on experiments with Poisson noise, and find that our method substantially outperforms its competitors. Finally, in Section 6, we use our method to regularize a correspondence analysis performed to understand how consumers perceive different perfumes.

5.1 Gaussian noise

We compare our estimators to existing ones by reproducing the simulations of Candès et al. [2013]. For this experiment, we generated data matrices of size 200×500 according to the Gaussian noise model (8) with four signal-to-noise ratios $\text{SNR} \in \{0.5, 1, 2, 4\}$ calculated as $1/(\sigma\sqrt{np})$, and two values for the underlying rank $k \in \{10, 100\}$. For each combination of SNR and k , we repeat the simulation 50 times and report median performance in Table 1.

Methods under consideration: In addition to our stable autoencoder (SA) as defined in (6) and iterated stable autoencoder (ISA) described in Algorithm 1, we also consider the following estimators:³

³As discussed in Section 2.1, we applied our stable autoencoding methods to X^\top rather than X , so that n was larger than p . For ISA, we ran the iterative Algorithm 1 for 100 steps, but the algorithm appeared to become stable after 10 steps already.

- Truncated SVD with fixed rank k (TSVD- k). This is the classical approach described in (2).
- Adaptively truncated SVD (TSVD- τ), using the asymptotically optimal threshold of Gavish and Donoho [2014a].
- Asymptotically optimal singular-value shrinkage (ASYMP) in the Marchenko-Pastur asymptotic regime given the Frobenius norm loss [Shabalin and Nobel, 2013, Gavish and Donoho, 2014b], with shrinkage function

$$\psi(d) = \begin{cases} \frac{1}{d} \sqrt{(d^2 - (1 + \beta) n \sigma^2)^2 - 4 \beta n^2 \sigma^4} & \text{for } d^2 \geq (1 + \sqrt{\beta})^2 n \sigma^2 \\ 0 & \text{else.} \end{cases} \quad (22)$$

- The shrinkage scheme of Verbanck et al. [2013] motivated by low-noise (LN) asymptotics. It uses for $\psi(d_l)$ in (3),

$$\psi(d_l) = \begin{cases} d_l \left(1 - \frac{\sigma^2}{d_l^2}\right) & \text{for } l \leq k \\ 0 & \text{else.} \end{cases} \quad (23)$$

- Singular value soft thresholding (SVST) [Cai et al., 2010], where the singular values are soft-thresholded by τ selected by minimizing a Stein unbiased risk estimate (SURE), as suggested by Candès et al. [2013]

All the estimators are defined assuming the variance of the noise σ^2 known. In addition, TSVD- k , SA, and LN require the rank k as a tuning parameter. In this case, we set k to the true rank of the underlying signal.

As our simulation study makes clear, the proposed methods have very different strengths and weaknesses. Both methods that apply a hard thresholding rule to the singular values, namely TSVD- k and TSVD- τ , provide accurate MSE when the SNR is high but break down

k	SNR	Stable		TSVD		ASYMP	SVST	LN
		SA	ISA	k	τ			
MSE								
10	4	0.004	0.004	0.004	0.004	0.004	0.008	0.004
100	4	0.037	0.036	0.038	0.038	0.037	0.045	0.037
10	2	0.017	0.017	0.017	0.016	0.017	0.033	0.017
100	2	0.142	0.143	0.152	0.158	0.146	0.156	0.141
10	1	0.067	0.067	0.072	0.072	0.067	0.116	0.067
100	1	0.511	0.775	0.733	0.856	0.600	0.448	0.491
10	0.5	0.277	0.251	0.321	0.321	0.250	0.353	0.257
100	0.5	1.600	1.000	3.164	1.000	0.961	0.852	1.477
Rank								
10	4		10		10	10	65	
100	4		100		100	100	193	
10	2		10		10	10	63	
100	2		100		100	100	181	
10	1		10		10	10	59	
100	1		29.6		38	64	154	
10	0.5		10		10	10	51	
100	0.5		0		0	15	86	

Table 1: Mean cell-wise squared error (top) and rank estimates (bottom) obtained by the methods described in Section 5.1. Best results linewise are indicated in bold.

in low SNR settings. Conversely, the SVST behaves well in low SNR settings, but struggles in other regimes. This is not surprising, as the method over-estimates the rank of μ . This behavior is reminiscent of what happens in lasso regression [Tibshirani, 1996] when too many variables are selected [Zou, 2006, Zhang and Huang, 2008].

Meanwhile, the estimators with non-linear singular-value shrinkage functions, namely SA, ISA, ASYMP, and LN are more flexible and perform well expect in the very difficult scenario where the signal is overwhelmed by the noise. Both ASYMP and ISA estimate the rank accurately except when the signal is nearly indistinguishable from the noise (SNR=0.5 and $k=100$).

5.2 Poisson noise

Once we move beyond the isotropic Gaussian case, our method can both learn better singular vectors and out-perform its competitors in terms of MSE. We illustrate this phenomenon with a simple simulation example, where we drew X of size $n = 50$ and $p = 20$ from a Poisson distribution with expectation μ of rank 3 represented in Figure 1. Because the three components of μ have different levels of concentration—the first component is rather diffuse, while the third one is concentrated in a corner—adapting to the Poisson variance structure is important.

We varied the effective signal-to-noise ratio by varying the mean number of counts in X , i.e., $N = \sum_{ij} \mu_{ij}$. We then report results for the normalized mean matrix μ/N . For each sample size, we applied the different estimators described in Section 2.2 on X to estimate μ . The SA and ISA estimators are computed by perturbing the data with Poisson noise, which is equivalent to using $\delta = 0.5$ in (18). We also used LN, ASYMP and TSVD- τ as baselines, although they are only formally motivated in the Gaussian model. These methods require a value for σ . For LN, we used the method recommended by Josse and Husson [2011]:

$$\hat{\sigma}^2 = \frac{\left\| X - \sum_{l=1}^k u_l d_l v_l \right\|_2^2}{np - nk - kp + k^2}. \quad (24)$$

For ASYMP and TSVD- τ , we used the estimator suggested in Gavish and Donoho [2014b]

$$\hat{\sigma} = \frac{d_{med}}{\sqrt{n\mu_\beta}}, \quad (25)$$

with d_{med} the median of the singular values of X and μ_β the median of the Marcenko-Pastur distribution.

In addition to providing MSE (Table 2), we also report the alignment of the row/column directions U and V with the true (Table 3). We measured alignment using the RV coefficient (Escoufier [1973]; see Josse and Holmes [2013] for a review), which is a correlation coefficient

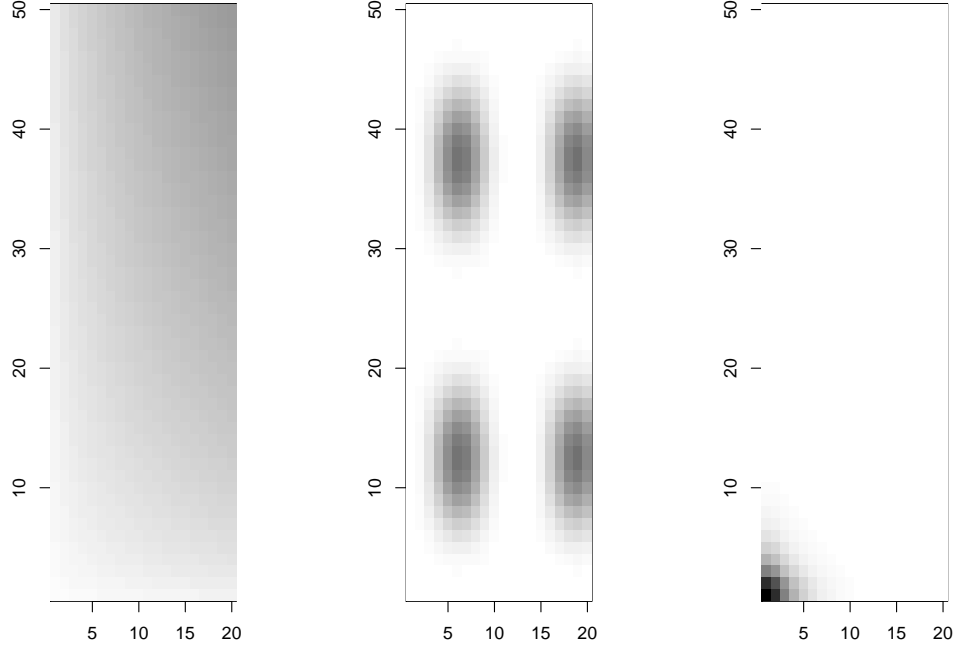


Figure 1: The 3 components of the mean of the underlying Poisson process; the dark areas have the highest intensity. The corresponding singular values have relative magnitudes 1.1 : 1.4 : 1.

between matrices that takes values between 0 and 1. Finally, we also give the estimated rank (Table 4.)

We see that our methods based on stable autoencoding do well across all noise levels. In the high-noise setting (i.e., with a small number of count observations N), the iterated stable autoencoder does particularly well, as it is able to use a lower rank in response to the weaker signal. As seen in Table 3, the ability to learn new singular vectors appears to have been useful here, as the “ \hat{U} ” and “ \hat{V} ” matrices obtained by stable autoencoding are much better aligned with the population ones than those produced by the SVD are. We also see that, in the low noise setting where N is large, ISA recovers the true rank $k = 3$

N	Stable		TSVD		ASYMP	LN
	SA	ISA	k	τ		
200	1.9	1.22	2.72	2.16	1.81	2.17
400	0.77	0.53	1.1	0.95	0.78	0.88
600	0.46	0.37	0.63	0.58	0.48	0.52
800	0.33	0.3	0.44	0.43	0.35	0.37
1000	0.25	0.24	0.32	0.33	0.27	0.28
1200	0.2	0.19	0.25	0.27	0.22	0.22
1400	0.16	0.16	0.2	0.22	0.19	0.18
1600	0.14	0.13	0.17	0.19	0.16	0.15
1800	0.12	0.11	0.14	0.16	0.14	0.13
2000	0.11	0.1	0.13	0.14	0.13	0.12

Table 2: Mean cell-wise squared error.

N	RV for U			RV for V		
	SVD	SA	ISA	SVD	SA	ISA
200	0.35	0.4	-	0.35	0.4	-
400	0.52	0.57	-	0.52	0.57	-
600	0.64	0.68	0.8	0.64	0.68	0.8
800	0.72	0.76	0.87	0.72	0.76	0.87
1000	0.78	0.82	0.89	0.78	0.82	0.89
1200	0.84	0.87	0.91	0.84	0.87	0.91
1400	0.88	0.9	0.92	0.88	0.9	0.92
1600	0.9	0.91	0.93	0.9	0.91	0.93
1800	0.92	0.93	0.94	0.92	0.93	0.94
2000	0.93	0.94	0.94	0.93	0.94	0.94

Table 3: RV coefficients between the estimated and true U and V matrices. For ISA, we only averaged performance over examples where the estimated rank was at least 3. In the $N = 200$ and $N = 500$ cases, no results are given for ISA since the estimated rank is always less than 3.

almost exactly, whereas ASYMP and TSVD- τ do not. Finally, we note that all shrinkage methods did better than the baseline, namely the simple rank-3 SVD. Thus, even though LN, ASYMP and TSVD- τ are only formally motivated in the Gaussian noise case, our results suggest that they are still better than no regularization on generic problems.

N	TSVD- τ	ASYMP	ISA
200	1.97	3.33	1.3
400	2.21	3.54	1.93
600	2.53	3.81	2.01
800	2.77	3.93	2.07
1000	2.95	3.98	2.28
1200	3.08	4.01	2.61
1400	3.15	4.05	2.86
1600	3.18	4.08	2.98
1800	3.21	4.09	3
2000	3.19	3.99	3

Table 4: Rank estimates.

6 Example: Perfume Data

Finally, we use stable autoencoding to regularize a sensory analysis of perfumes. The data for the analysis was collected by asking consumers to describe 12 luxury perfumes such as *Chanel Number 5* and *J'adore* with words. The answers were then organized in a 12×39 (39 words unique were used) data matrix where each cell represents the number of times a word is associated to a perfume; a total of $N = 1075$ were used overall. The dataset is available at <http://factominer.free.fr/docs/perfume.txt>. We used correspondence analysis (CA) to visualize the associations between words and perfumes. Here, the technique allows to highlight perfumes that were described using a similar profile of words, and to find words that describe the differences between groups of perfumes.

In order to get a better idea of which regularization method is the most trustworthy here, we ran a small bootstrap simulation study built on top of the perfume dataset. We used the full $N = 1075$ perfume dataset as the population dataset, and then generated samples of size $N = 200$ by subsampling the original dataset without replacement. Then, on each sample, we performed a classical correspondence analysis by performing a rank- k truncated SVD of the matrix M (16), as well as several regularized alternatives described in Section

	d_1	d_2	RV row	RV col	k
TRUE	0.44	0.15			
CA	0.62	0.42	0.41	0.72	
LN	0.28	0.11	0.47	0.79	
SA	0.34	0.18	0.50	0.79	
ISA	0.40	0.18	0.52	0.81	2.43

Table 5: Performances of standard correspondence analysis (CA) as well as regularized alternatives on the perfume dataset. We report singular values, RV-coefficients and rank estimates; Results correspond to the mean over the 1000 simulations.

5.1.

For each estimator, we report its singular values, as well as the RV-coefficients between its row (respectively column) coordinates and the population ones. All the methods except for ISA require us to specify the rank k as an input parameter. Here, of course, k is unknown since we are working with a real dataset; however, examining the full-population dataset suggests that using $k = 2$ components is appropriate. For LN, SA and ISA, we set tuning parameters as in Section 5.2, namely LN uses $\hat{\sigma}$ from (24), while SA is performed with $\delta = 0.5$. For ISA we used $\delta = 0.3$; this latter choice was made to get rank-2 estimates. In practice, one could also consider cross-validation to find a good value for δ .

Results are shown in Table 5. From a practical point of view, it is also interesting to compare the graphical output of correspondence analysis with and without regularization. Figure 2 (top) shows two-dimensional CA representation on one sample and Figure 2 (bottom) shows the representation obtained with ISA. Only, the 20 words that contribute the most to the first two dimensions are represented. The analysis is performed using the R package FactoMineR [Lê et al., 2008].

Our results emphasize that, although correspondence analysis is often used as a visualization technique, appropriate regularization is still important, as regularization may substantially affect the graphical output. For example, on the basis of the CA plot, the per-

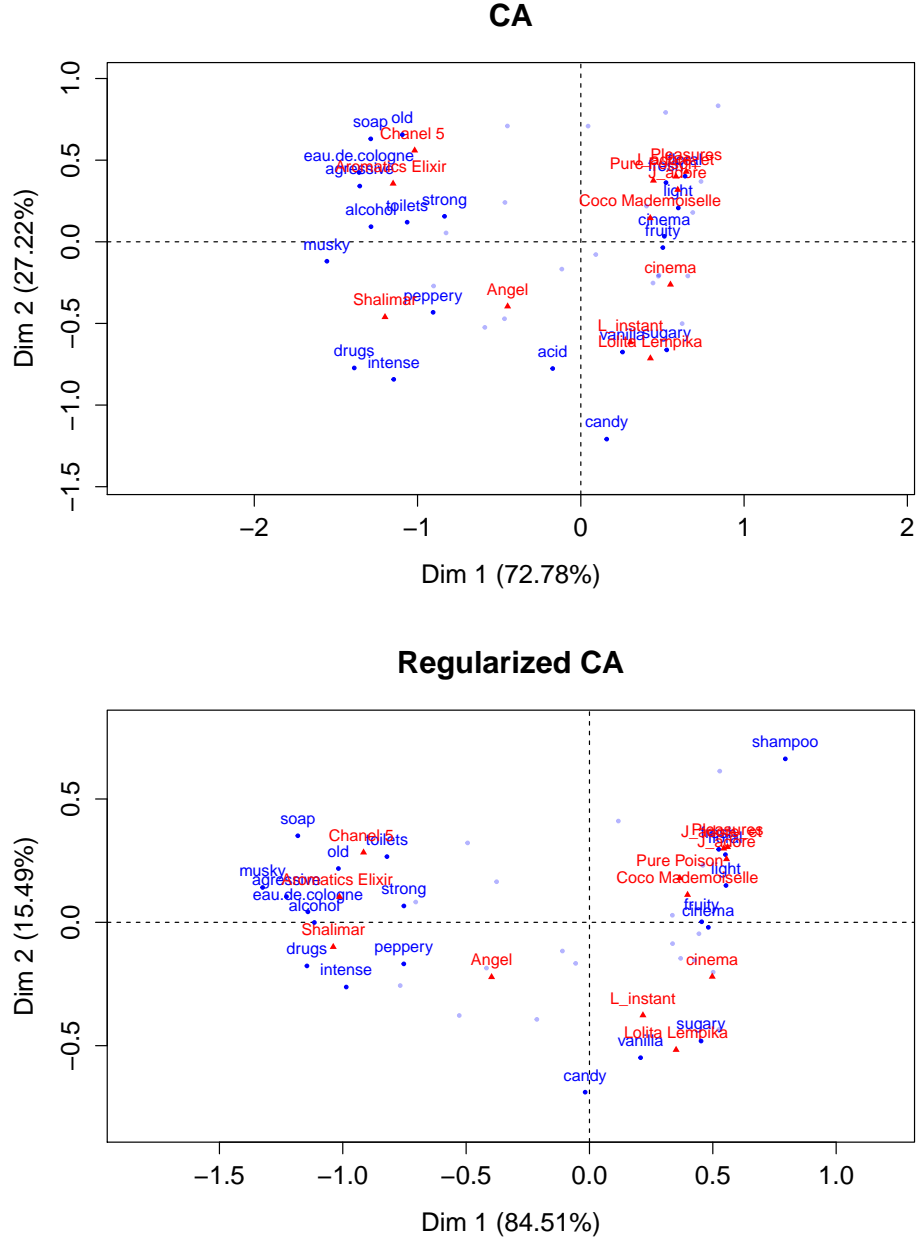


Figure 2: Results for CA on a sample data set (top) and Regularized CA (bottom) using ISA on a single subsample of size $N = 200$. Only the 20 words that contribute the most to the dimensions of variability are represented.

fume *Shalimar* looks like an outlier, whereas after regularization it seems to fit in a cluster with *Chanel 5* and *Elixir*. We know from Table 5 that the regularized CA plots are better aligned with the population ones than the unregularized ones are; thus, we may be more inclined to trust insights from the regularized analysis.

7 Discussion

In this paper, we introduced a new framework for low-rank matrix estimation that works by transforming noise models into regularizers via a parametric bootstrap. Our method can adapt to non-isotropic noise structures, thus enabling it to substantially outperform its competitors on problems with, e.g., Poisson noise.

At a high level, our framework works by creating pseudo-datasets \tilde{X} from X using the noise model $\mathcal{L}(X)$. If two pseudo-datasets \tilde{X}_1 and \tilde{X}_2 are both likely given $\mathcal{L}(X)$, then we want the induced mean estimates $\tilde{\mu}_k^1 = \tilde{X}_1 \hat{B}_k$ and $\tilde{\mu}_k^2 = \tilde{X}_2 \hat{B}_k$ to be close to each other. The stable autoencoder (6) enables us to turn this intuition into a concrete regularizer by using a parametric bootstrap. It remains to be seen whether this idea of regularization via bootstrapping pseudo-datasets can be extended to other classes of low-rank matrix algorithms, as discussed by, e.g., Udell et al. [2014].

Acknowledgment

The authors are grateful for helpful conversations with Brad Efron, David Donoho, and Will Fithian. Part of this work was performed while J.J. was visiting Stanford University, with support from an AgreeSkills fellowship of the European Union Marie-Curie FP7 CO-FUND People Programme. S.W. is supported by a B.C. and E.J. Eaves Stanford Graduate

Fellowship.

References

- Jinho Baik and Jack W Silverstein. Eigenvalues of large sample covariance matrices of spiked population models. *Journal of Multivariate Analysis*, 97(6):1382 – 1408, 2006.
- Pierre Baldi and Kurt Hornik. Neural networks and principal component analysis: Learning from examples without local minima. *Neural Networks*, 2(1):53–58, 1989.
- Pierre Baldi and Peter Sadowski. The dropout learning algorithm. *Artificial Intelligence*, 210:78–122, 2014.
- Chris M Bishop. Training with noise is equivalent to Tikhonov regularization. *Neural Computation*, 7(1):108–116, 1995.
- Hervé Bouchard and Yves Kamp. Auto-association by multilayer perceptrons and singular value decomposition. *Biological Cybernetics*, 59(4-5):291–294, 1988.
- Jian-Feng Cai, Emmanuel J Candès, and Zuowei Shen. A singular value thresholding algorithm for matrix completion. *SIAM Journal on Optimization*, 20(4):1956–1982, 2010.
- Emmanuel J Candès and Terence Tao. The power of convex relaxation: Near-optimal matrix completion. *IEEE Transactions on Information Theory*, 56(5):2053–2080, 2010.
- Emmanuel J Candès, Carlos A Sing-Long, and Joshua D Trzasko. Unbiased risk estimates for singular value thresholding and spectral estimators. *IEEE Transactions on Signal Processing*, 61(19):4643–4657, 2013.
- Sourav Chatterjee. Matrix estimation by universal singular value thresholding. *To appear in the Annals of Statistics*, 2014.
- Bradley Efron and Robert Tibshirani. *An Introduction to the Bootstrap*. Chapman & Hall/CRC, 1993.
- Yves Escoufier. Le traitement des variables vectorielles. *Biometrics*, 29:751–760, 1973.
- Matan Gavish and David L Donoho. The optimal hard threshold for singular values is $4/\sqrt{3}$. *IEEE Transactions on Information Theory*, 60(8), 2014a.
- Matan Gavish and David L Donoho. Optimal shrinkage of singular values. *arXiv:1405.7511v2*, 2014b.
- Amir Globerson and Sam Roweis. Nightmare at test time: robust learning by feature deletion. In *Proceedings of the International Conference on Machine Learning*, 2006.
- Ian Goodfellow, David Warde-farley, Mehdi Mirza, Aaron Courville, and Yoshua Bengio. Maxout networks. In *Proceedings of the 30th International Conference on Machine Learning*, pages 1319–1327, 2013.
- Michael J Greenacre. *Theory and Applications of Correspondence Analysis*. Academic Press, 1984.

- Michael J Greenacre. *Correspondence Analysis in Practice, Second Edition*. Chapman & Hall, 2007.
- Ian Johnstone. On the distribution of the largest eigenvalue in principal components analysis. *The Annals of Statistics*, 29(2):295–327, 2001.
- Ian Jolliffe. *Principal Component Analysis*. Springer, 2002.
- Julie Josse and Susan Holmes. Measures of dependence between random vectors and tests of independence. literature review. *arXiv preprint arXiv:1307.7383*, 2013.
- Julie Josse and François Husson. Selecting the number of components in PCA using cross-validation approximations. *Computational Statistics and Data Analysis*, 56(6):1869–1879, 2011.
- Julie Josse and Sylvain Sardy. Adaptive shrinkage of singular values. *To appear in Statistics and Computing*, 2014.
- Yehuda Koren, Robert Bell, and Chris Volinsky. Matrix factorization techniques for recommender systems. *Computer*, 42(8):30–37, 2009.
- Alex Krizhevsky, Ilya Sutskever, and Geoffrey E Hinton. Imagenet classification with deep convolutional neural networks. In *Advances in Neural Information Processing Systems*, pages 1097–1105, 2012.
- Sébastien Lê, Julie Josse, and François Husson. FactoMineR: An R package for multivariate analysis. *Journal of Statistical Software*, 25(1):1–18, 2008.
- Jeffrey T Leek and John D Storey. Capturing heterogeneity in gene expression studies by surrogate variable analysis. *PLoS genetics*, 3(9):e161, 2007.
- Michael Lustig, David L Donoho, Juan M Santos, and John M Pauly. Compressed sensing MRI. *Signal Processing Magazine, IEEE*, 25(2):72–82, 2008.
- Debashis Paul. Asymptotics of sample eigenstructure for a large dimensional spiked covariance model. *Statistica Sinica*, 17(4):1617, 2007.
- Alkes L Price, Nick J Patterson, Robert M Plenge, Michael E Weinblatt, Nancy A Shadick, and David Reich. Principal components analysis corrects for stratification in genome-wide association studies. *Nature Genetics*, 38(8):904–909, 2006.
- Andrey A Shabalin and Andrew B Nobel. Reconstruction of a low-rank matrix in the presence of Gaussian noise. *Journal of Multivariate Analysis*, 118:67–76, 2013.
- Patrice Y Simard, Yann A Le Cun, John S Denker, and Bernard Victorri. Transformation invariance in pattern recognition: Tangent distance and propagation. *International Journal of Imaging Systems and Technology*, 11(3):181–197, 2000.
- Nitish Srivastava, Geoffrey Hinton, Alex Krizhevsky, Ilya Sutskever, and Ruslan Salakhutdinov. Dropout: A simple way to prevent neural networks from overfitting. *The Journal of Machine Learning Research*, 15(1):1929–1958, 2014.
- Yoshio Takane. *Constrained Principal Component Analysis and Related Techniques*. Chapman & Hall, 2013.

- Robert Tibshirani. Regression shrinkage and selection via the lasso. *Journal of the Royal Statistical Society. Series B (Methodological)*, pages 267–288, 1996.
- Madeleine Udell, Corinne Horn, Reza Zadeh, and Stephen Boyd. Generalized low rank models. *arXiv preprint arXiv:1410.0342*, 2014.
- Laurens van der Maaten, Minmin Chen, Stephen Tyree, and Kilian Q Weinberger. Learning with marginalized corrupted features. In *Proceedings of the International Conference on Machine Learning*, 2013.
- Marie Verbanck, Julie Josse, and François Husson. Regularised PCA to denoise and visualise data. *Statistics and Computing*, pages 1–16, 2013.
- Stefan Wager, Sida Wang, and Percy Liang. Dropout training as adaptive regularization. In *Advances in Neural Information Processing Systems*, pages 351–359, 2013.
- Stefan Wager, William Fithian, Sida Wang, and Percy Liang. Altitude training: Strong bounds for single-layer dropout. In *Advances in Neural Information Processing Systems*, 2014.
- Sida I Wang, Mengqiu Wang, Stefan Wager, Percy Liang, and Christopher D Manning. Feature noising for log-linear structured prediction. In *Empirical Methods in Natural Language Processing*, 2013.
- C. H. Zhang and J. Huang. The sparsity and bias of the lasso selection in high-dimensional linear regression. *The Annals of Statistics*, 36(4):1567–1594, 2008.
- H. Zou. The adaptive LASSO and its oracle properties. *Journal of the American Statistical Association*, 101:1418–1429, 2006.

A Proofs

Proof of Theorem 1. We begin by establishing the equivalence between (6) and (9). By bias-variance decomposition, we can check that

$$\begin{aligned}\mathbb{E}_{\varepsilon_{ij} \stackrel{\text{iid}}{\sim} \mathcal{N}(0, \sigma^2)} \left[\|X - (X + \varepsilon) B\|_2^2 \right] &= \|X - XB\|_2^2 + \mathbb{E}_\varepsilon \left[\|\varepsilon B\|_2^2 \right] \\ &= \|X - XB\|_2^2 + \sum_{i,j,k} \text{Var} [\varepsilon_{ij}] B_{jk}^2 \\ &= \|X - XB\|_2^2 + n\sigma^2 \|B\|_2^2,\end{aligned}$$

and so the two objectives are equivalent.

To show that $\hat{\mu}_k^{\text{stable}}$ can be written as (10), we solve for $\hat{\mu}_k^{\text{stable}} = X\hat{B}_k$ explicitly, where

$$\hat{B}_k = \underset{B}{\text{argmin}} \left\{ \|X - XB\|_2^2 + \lambda \|B\|_2^2 : \text{rank}(B) \leq k \right\}.$$

Let $X = UDV^\top$ be the SVD of X . For any matrix M of the same dimension as D , $\|UMV^\top\|_2^2 = \|M\|_2^2$. Thus, we can equivalently write the problem

$$\hat{B}_k = V\tilde{B}_kV^\top, \text{ where } \tilde{B}_k = \underset{B}{\text{argmin}} \left\{ \|D - DB\|_2^2 + \lambda \|B\|_2^2 : \text{rank}(B) \leq k \right\}.$$

Now, because D is diagonal, $(DB)_{ij} = D_{ii}B_{ij}$. Thus, we conclude that $\tilde{B}_{ij} = 0$ for all $i \neq j$, while the problem separates for all the diagonal terms. Without the rank constraint on B , we find that the diagonal terms \tilde{B}_{ii} are given by

$$\tilde{B}_{ii} = \underset{B_{ii}}{\text{argmin}} \left\{ (1 - B_{ii})^2 D_{ii}^2 + \lambda \tilde{B}_{ii}^2 \right\} = \frac{D_{ii}^2}{\lambda + D_{ii}^2}.$$

Meanwhile, we can check that adding the rank constraint amounts to zeroing out all but the k largest of the \tilde{B}_{ii} . Thus, plugging this into our expression of $\hat{\mu}$, we get that

$$\hat{\mu}_k^{\text{stable}} = \sum_{i=1}^k U_i \cdot \frac{D_{ii}}{1 + \lambda/D_{ii}^2} V_i^\top.$$

□

Proof of Theorem 2. We start by showing that \widehat{B} is the solution to the unconstrained version of (11). Let V be a matrix defined by

$$V_{ij} = \text{Var}_{\tilde{X} \sim \mathcal{L}(X)} [\tilde{X}_{ij}].$$

Because \tilde{X} has mean X , we can check that

$$\mathbb{E}_{\tilde{X} \sim \mathcal{L}(X)} \left[\left\| X - \tilde{X}B \right\|_2^2 \right] = \|X - XB\|_2^2 + \sum_{i,j,k} V_{ij} B_{jk}^2.$$

Thus,

$$\frac{1}{2} \frac{\partial}{\partial B_{jk}} \mathbb{E}_{\tilde{X} \sim \mathcal{L}(X)} \left[\left\| X - \tilde{X}B \right\|_2^2 \right] = - \sum_i X_{ij} (X - XB)_{ik} + \sum_i V_{ij} B_{jk}.$$

Setting gradients to zero, we find an equilibrium

$$X^\top X = X^\top XB + SB, \text{ where } S_{jk} = \begin{cases} \sum_{i=1}^n V_{ij} & \text{for } j = k, \\ 0 & \text{else.} \end{cases}$$

Thus, we conclude that

$$\widehat{B} = (X^\top X + S)^{-1} X^\top X$$

is in fact the solution to (11) without the rank constraint.

Next, we show how we can get from \widehat{B} to \widehat{B}_k using (13). For any matrix B , we can verify by quadratic expansion that

$$\begin{aligned} \|X - XB\|_2^2 &= \|X - X\widehat{B}\|_2^2 + \|X(\widehat{B} - B)\|_2^2 + 2 \text{tr} \left((X - X\widehat{B})^\top (X\widehat{B} - XB) \right) \\ &= \|X - X\widehat{B}\|_2^2 + \|X(\widehat{B} - B)\|_2^2 \\ &\quad + 2 \text{tr} \left(X^\top X (X^\top X + S)^{-1} X^\top X - X^\top X \right) (B - \widehat{B}) \end{aligned}$$

Meanwhile,

$$\begin{aligned} \|S^{\frac{1}{2}} B\|_2^2 &= \|S^{\frac{1}{2}} \widehat{B}\|_2^2 + \|S^{\frac{1}{2}} (B - \widehat{B})\|_2^2 + 2 \text{tr} \left(\widehat{B}^\top S (B - \widehat{B}) \right) \\ &= \|S^{\frac{1}{2}} \widehat{B}\|_2^2 + \|S^{\frac{1}{2}} (B - \widehat{B})\|_2^2 + 2 \text{tr} \left(X^\top X (X^\top X + S)^{-1} S (B - \widehat{B}) \right). \end{aligned}$$

Summing everything together, we find that

$$\|X - XB\|_2^2 + \|S^{\frac{1}{2}}B\|_2^2 = \|X(B - \widehat{B})\|_2^2 + \|S^{\frac{1}{2}}(B - \widehat{B})\|_2^2 + R(\widehat{B}, X)$$

where R is a residual term that does not depend on B . Thus, we conclude that

$$\begin{aligned}\widehat{B}_k &= \operatorname{argmin}_B \left\{ \|X - XB\|_2^2 + \|S^{\frac{1}{2}}B\|_2^2 : \operatorname{rank}(B) \leq k \right\} \\ &= \operatorname{argmin}_B \left\{ \operatorname{tr} \left((B - \widehat{B})^\top (X^\top X + S) (B - \widehat{B}) \right) : \operatorname{rank}(B) \leq k \right\}.\end{aligned}$$

As shown in, e.g., Takane [2013], we can solve this last problem by taking the top k terms of the eigendecomposition of $\widehat{B}^\top (X^\top X + S)^{-1} \widehat{B}$. \square

Proof of Theorem 3. For iterates $t = 0, 1, \dots$, define $M_t = \hat{\mu}_t^\top \hat{\mu}_t$. Here, we will show that M_t converges to a fixed point M^* , and that $M^* \preceq X^\top X$; the desired conclusion then follows immediately. First, by construction, we have that

$$M_0 = X^\top X \quad \text{and} \quad M_1 = X^\top X (X^\top X + S)^{-1} X^\top X (X^\top X + S)^{-1} X^\top X,$$

and so we immediately see that $M_1 \preceq M_0$. The general update for M_t is

$$M_{t+1} = g(M_t)^\top g(M_t), \quad \text{where } g(M) = \Sigma^{\frac{1}{2}}(M + S)^{-1}M, \quad (26)$$

where $\Sigma^{\frac{1}{2}}$ is a positive semi-definite solution to $(\Sigma^{\frac{1}{2}})^\top \Sigma^{\frac{1}{2}} = X^\top X$. Now, because matrix inversion is a monotone decreasing function over the positive semi-definite cone and $S \succ 0$, we find that

$$g(M) = \Sigma^{\frac{1}{2}} \left(I - (M + S)^{-1} S \right)$$

is monotone increasing in M over the positive semi-definite cone. In particular

$$\text{if } M_t \preceq M_{t-1}, \text{ then } M_{t+1} \preceq M_t.$$

By induction, the sequence M_t is monotone decreasing with respect to the positive semi-definite cone order; by standard arguments, it thus follows that this sequence must converge to a limit M^* . \square

Proof of Theorem 4. As in the proof of Theorem 3, let $M^* = \hat{\mu}^\top \hat{\mu}$. Because M^* is a fixed point, we know that

$$M^* = M^* (M^* + S)^{-1} X^\top X (M^* + S)^{-1} M^*.$$

Now, because M^* is symmetric with eigenvector u , we can decompose it as

$$M^* = M^\perp + \lambda_u u u^\top, \text{ where } \lambda_u = u^\top M^* u \text{ and } \|M^\perp u\|_2 = 0.$$

By combining these equalities and using the monotonicity of matrix inversion, we find that

$$\begin{aligned} \lambda_u &= u^\top M^* u \\ &= \lambda_u^2 u^\top (M^* + S)^{-1} X^\top X (M^* + S)^{-1} u \\ &\leq \lambda_u^2 u^\top S^{-1} X^\top X S^{-1} u. \end{aligned}$$

This relation can only hold if $\lambda_u = 0$, or $1 \leq \lambda_u u^\top S^{-1} X^\top X S^{-1} u$, and so our desired conclusion must hold. \square